"Heisenberg microscope" decoherence atom interferometry

John F. Clauser and Shifang Li
Physics Department, University of California–Berkeley, Berkeley, California 94720
(Received 1 November 1993)

Atom de Broglie–wave interference fringes are revealed by their selective destruction. A thermal potassium beam is transmitted through a Talbot-Lau atom interferometer. Different fringe Fourier components resonate in the interferometer at different atomic velocities. The thermal velocity distribution averages and washes out the high-frequency components. ac-modulated laser light passes through the interferometer, is scattered by atoms at one velocity, and destroys, and thereby reveals via the ac modulation, the associated high-frequency fringe contribution.

PACS number(s): 03.75.Dg, 35.80.+s, 42.50.Wm, 42.50.Vk

An argument by Heisenberg [1] is commonly cited to illustrate the uncertainty principle. Consider an attempt to determine the position of a particle with a well-defined momentum by scattering a single photon off of it and then viewing the scattered photon with a microscope. The scattering imparts an uncertain momentum recoil to the atom. The product of this momentum uncertainty with the position resolution of the microscope satisfies the uncertainty principle. Thus two microscopes separated along an atom's propagation path cannot localize it in phase space any more finely than the limit set by the uncertainty principle.

Recently, Walls *et al.* [2] analyzed an analogous problem for freely propagating atoms with well-defined momenta that form de Broglie–wave fringes in a Young's two-slit interferometer. They consider a situation wherein both slits are simultaneously illuminated with light that is resonant with an atomic transition and calculate the resulting atomic fringe visibility as a function of slit separation. They predict that when the slits are separated sufficiently, so that a Heisenberg microscope viewing the reemitted fluorescence can image this light to determine which slit an atom passes, then the atomic fringe visibility will vanish. But when the slit spacing is comparable to the optical wavelength, such a determination by the microscope exceeds its resolving power and then the interference pattern will persist. Further, the presence of the microscope is unnecessary for the predicted visibility dependence on slit spacing to obtain. Only the microscope's illumination need be present.

Recently, atom de Broglie–wave versions of Young's two-slit experiment have been performed [3], along with other more efficient forms of atom interferometry experiments [4–6]. The above predictions can be tested using atom interferometry. Indeed, Sterr *et al.* [6] destroyed atom interference fringes by passing high-intensity resonant laser light through their atom interferometer. In that experiment many photons were scattered off of each atom and although their atomic paths have an amplitude for being physically separated in space, the paths are continuously distributed in space and are not clearly localized by a scattering event. It is the purpose of the present work to describe the results of an atom interferometry experiment which demonstrates destruction of atom interference fringes by the scattering of a single low-energy photon by an atom, such that the atom's path could be localized by the scattering. Given our multiply connected geometry, a localized atom can pass through only one slit. Nonetheless, in our experiment amplitudes for an atom's passage simultaneously through more than one physically different slit provide quantum interference when no scattering occurs. We note that both our experiment and that by Sterr *et al.* probe only the regime wherein the atomic path separation is greater than the optical wavelength, while the predicted persistence of fringes at narrow atomic path spacing remains to be demonstrated.

In our experiment spatial de Broglie–wave interference of potassium atoms is revealed by its selective destruction. A thermal potassium beam is transmitted through a velocity-selective atom interferometer and detected. The interferometer consists of a sequence of three vacuum-slit diffraction gratings. Quantum interference fringes are formed on the third grating and are masked by the grating, thereby determining the interferometer's transmitted atomic current. Atoms at characteristic resonant atomic velocities and/or de Broglie wavelengths form fringe patterns that contain high-spatial-frequency Fourier components. The thermal velocity distribution produces an average over these components that washes out and hides the high-frequency fringes. ac-modulated laser light passes through the interferometer, near the middle grating. Since imaging of the fluorescent light *could* be used to determine which slit an atom passes, the contribution to the averaged pattern by atoms at the laser's Doppler-shifted wavelength is removed. That component is thus ac modulated and detected.

The apparatus (shown in Fig. 1) is a modification of one previously described by the authors [4]. An upward directed thermal beam of potassium atoms is produced by a 450 K isothermal oven with 200 μm$\times$5 mm knife-edge exit slits. Atoms pass through a 300 μm$\times$8 mm collimating slit, a cold baffle, a differential pumping (DP) slit, and thence through an atom interferometer. The interferometer operates at 10^{-9} Torr, adjacent a second cold baffle that limits the background potassium density. It consists of a sequence of three rectangular 1-μm-thick planar silicon-nitride diffraction gratings G_1, G_2, and G_3,

each cut by 8.5-mm-long parallel slits. Grating planes are separated by $R_{1,2}=46.2$ cm. There are 22 slits in G_1, 76 in G_3, and 111 in G_2, periodically spaced at associated periods $a_1=a_3=16.2$ μm and $a_2=8.1$ μm, respectively. All gratings have an open fraction of about $(\mathscr{s}/a)=\frac{1}{8}$, where $\mathscr{s}$ is the slit width. Grating alignment is done using a He-Ne laser passing through the gratings (and through an auxiliary grating on the G_2 plane). Transmitted atoms are ionized on a rhenium hotwire. The resulting analog ion current is electro-statically focused onto an electron multiplier and amplified. The whole system is vibrationally isolated from the floor and is stationary relative to an inertial frame to a fraction of a micrometer during the transit time of a low-velocity atom through the interferometer.

Since an actual microscope is unnecessary for the experiments, none is included. "Microscope illumination" consists of a ribbon-shaped laser beam passing through the interferometer at near antiparallel incidence (20°) to the beam, immediately below G_2. It is circularly polarized, highly attenuated, has a bandwidth of about 15 MHz, and is produced by a single-mode diode laser at 766 nm. To determine the laser's tuning, we redirect it unattenuated at perpendicular incidence. Then, when the laser is tuned to a Doppler-free hyperfine resonance, deflection of the whole beam produces a dip in the transmitted beam current.

The laser is ac modulated at an audio frequency. The modulation wave form is divided into three periods. The first period is used to lock the laser wavelength to a resonance line of a potassium absorption cell. During the second (on) period, the laser is tuned to resonate with atoms at a desired velocity. ^{39}K atoms in the $F=1$ and 2 hyperfine levels with velocities $v_{F=1}$ and $v_{F=2}$, respectively, will be resonant when the laser's frequency ν satisfies the relations

$$v_{F=1}=(\nu-\nu_{F=1})\lambda/\cos(20°)\ ,$$
$$v_{F=2}=v_{F=1}-351\ \text{m/sec}\ , \tag{1}$$

where $\nu_{F=1}$ is the resonant frequency for zero velocity $F=1$ atoms and λ is the laser's wavelength. $F=2$ atoms will be resonant only for tunings with $v_{F=1}$ greater than 351 m/sec, the velocity equivalent of the hyperfine resonance spacing. During the third (off) period the laser is returned to an off-resonant (negative velocity) condition for all atoms. The dc ionized current from the full thermal beam through the interferometer is about 10–100 pA. The ac component of the transmitted atomic current (about 0.1% of the dc current at low-velocity tuning) is synchronously detected by integrating the current positively during the on period and negatively during the off period. Both the dc and ac are recorded as a function of grating position or laser tuning.

When the laser is off, de Broglie–wave fringes are formed in the interferometer via a generalization of the Talbot and Lau effects [7,4]. Figure 2 shows the associated calculated transmission probability $T_{\text{off}}(v,\Delta x)$ as a function of atomic velocity v and lateral grating displacement Δx (for half a period). We calculate the laser-on transmission probability $T_{\text{on}}(v,\Delta x)$, assuming a kinematical scattering near G_2 of one photon by each atom, assuming a classical atomic trajectory, and using the pointwise momentum-transfer photon scattering model

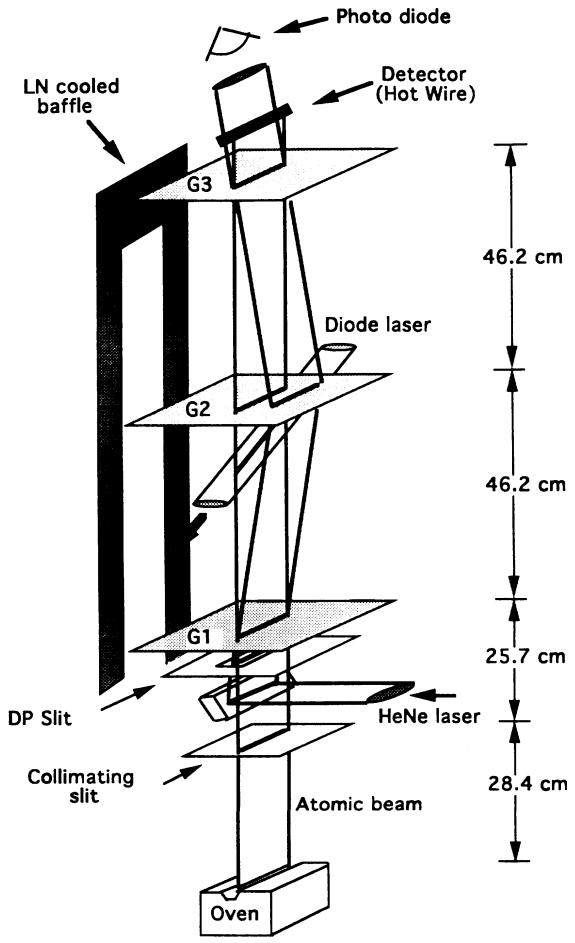

FIG. 1. Geometry of the experimental apparatus. The photomultiplier to measure fluorescence intensity is not shown.

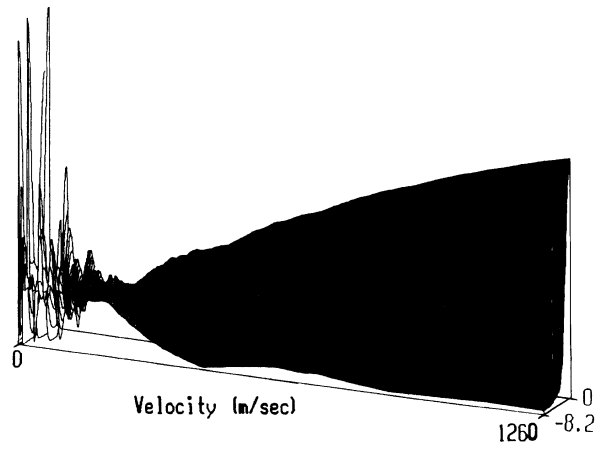

FIG. 2. Calculated laser-off interferometer transmission probability plotted as a function of atomic velocity and grating displacement. The periodic dependence on displacement is plotted through one-half of a geometric-shadow spacing period.

developed by Einstein [8] in his discussion of the kinematics required for thermal equilibrium to obtain when a gas is irradiated by thermal light. We first consider a line source of atoms at G_1 and the scattering of one incident circularly polarized photon near G_2, and then calculate the transmission by a single G_2 slit of width $\mathscr{s}_2$. The resulting probability for atoms at the G_3 lateral position x_3 is given by

$$I_1(x_3) \propto [9\xi^2 x - (x - x_3)^3]_{x=-\min(\mathscr{s}_2, -x_3+\xi)}^{x=\min(\mathscr{s}_2, x_3+\xi)} . \quad (2)$$

Here ξ is the maximum kinematically allowed scattering distance at G_3. It is proportional to the ratio of the photon and atom momenta via $\xi \equiv R_2 h\nu/Mvc$. Summing I_1 over the various slits in G_1, G_2, G_3 and averaging over the associated G_1 and G_3 slit widths yields the laser-on transmission probability $T_{on}(v, \Delta x)$, given the scattering of one photon. It is shown in Fig. 3. The hyperfine structure effectively limits the number of scatterings per atom to about one via the high probability that following a scattering the atom will optically pump and thereafter be transparent to the laser radiation. To further ensure only one scattering per atom in an atom's flight time through the laser beam and to provide a narrow effective laser bandwidth, the laser is attenuated heavily.

Since the laser is resonant with only a trivial number of atoms within the beam, we neglect its effect in calculating the transmitted dc atomic current, yielding

$$I_{dc}(\Delta x) \propto \int_0^\infty T_{off}(v, \Delta x) f(v) dv , \quad (3)$$

where $f(v)$ is the thermal velocity distribution of atoms in the beam. The transmitted ac current, correspondingly is given by

$$I_{ac}(\Delta x, \nu) \propto \int_0^\infty [T_{on}(v, \Delta x) - T_{off}(v, \Delta x)] \times p(v, \nu) f(v) dv , \quad (4)$$

where $p(v, \nu)$ is the probability that an atom will scatter one (and only one) photon in an atom's transit through

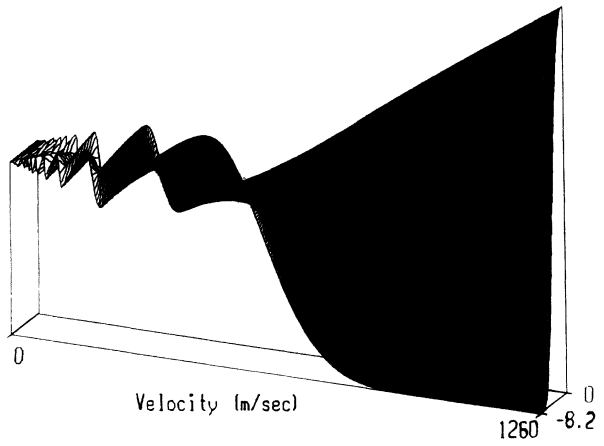

FIG. 3. Calculated laser-on interferometer transmission probability, given the scattering of one photon near G_2, plotted with the format of Fig. 2.

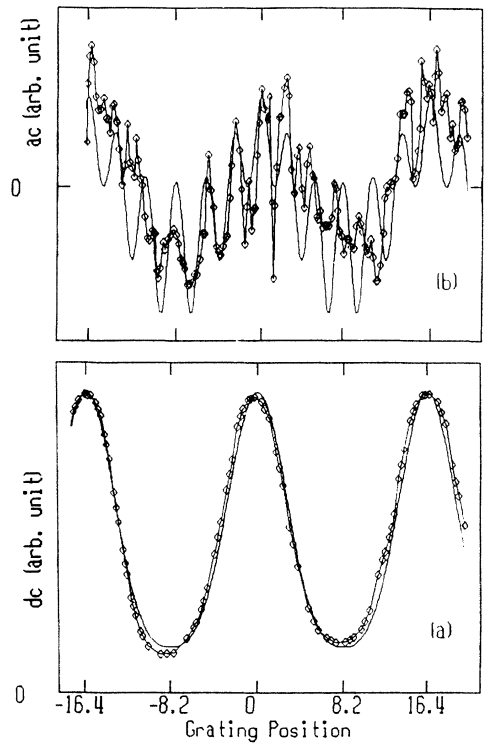

FIG. 4. Calculated and observed (diamond points) atomic currents as a function of grating relative displacement, Δx (μm). (a) The dc signal due to thermal beam illumination and (b) the ac signal showing the destroyed fringes for atoms at 211 m/sec.

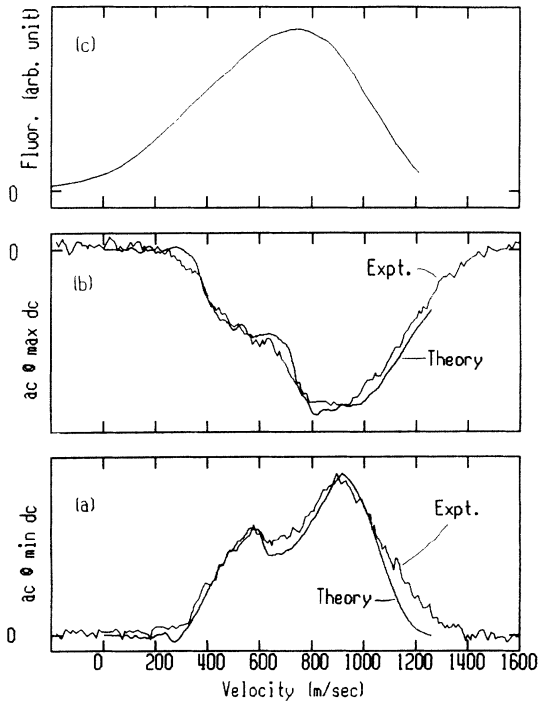

FIG. 5. (a) Calculated and (b) observed atomic current as a function laser tuning, in terms of $v_{F=1}$ [via Eq. (1)], for fixed grating relative displacement. (a) The ac at minimum dc and (b) at maximum dc. (c) Fluorescence intensity as a function laser tuning $v_{F=1}$.

the laser beam. It has two resonant near-Lorentzian components separated by 351 m/sec, corresponding to and weighted by the thermal populations 40% $F=1$ and 60% $F=2$.

To observe interference fringes, the laser is tuned to resonate with $F=1$ atoms at a velocity of 211 m/sec, i.e., 6 times the Talbot-Rayleigh velocity $v_{TR} \approx 35$ m/sec, corresponding to ac fringes at the sixth spatial harmonic of the geometric shadow period. While holding the laser tuning constant, the middle grating, G_2, is scanned laterally with a piezoelectric translator and the dc and ac signals are recorded simultaneously. These signals are shown as a function of grating displacement Δx in Figs. 4(a) and 4(b), along with the dc and ac calculated via Eqs. (3) and (4). (To give better agreement between the observed and calculated ac patterns, a small dc signal cross-talk component is added to the calculated ac signal.) Admittedly, the ac signal is quite noisy, as its signal-to-noise ratio is limited by the shot noise of the much larger dc. Nonetheless, the sixth spatial harmonic associated with the Talbot–von Lau resonance is evident in the data.

To observe the velocity dependence of the ac signal, the grating positions are held fixed and the laser tuning is swept. The measured signals obtained when the gratings are positioned for minimum and maximum transmitted dc are shown in Figs. 5(a) and 5(b), along with the calculated signals. Agreement between the calculated and measured signals appears to be quite good. For comparison, in Fig. 5(c) we show the laser excited fluorescence intensity measured using a photomultiplier and the same laser incidence angle (but with no gratings present) in response to a similar laser frequency scan.

We note that the hyperfine structure is not resolved in the fluorescence spectrum. By contrast, the transmission spectrum of Fig. 5(a) displays two well-resolved peaks whose spacing corresponds to the hyperfine structure. Evidently we have constructed what amounts to an atom interference filter whose velocity selectivity allows us to narrow the effective transmitted velocity range so as to provide an improvement in the optical spectral resolution. When the gratings are positioned for minimum dc transmission, then neither the laser-on nor laser-off conditions transmit atoms at high velocity. However, the reasons for these high-velocity cutoffs differ. In the laser-on condition only low-velocity atoms have sufficient scattering angle to reach a G_3 open slit. A cutoff then occurs at $\xi = a_3/2$, i.e., at an atomic velocity of about 740 m/sec. In the laser-off condition only atoms with velocities below $(\lambda_2/a_2)v_{TR} = 278$ m/sec have sufficiently long de Broglie wavelength so that two adjacent G_2 slits produce overlapping constructive interference at an open G_3 slit. The different cutoff velocities (and profiles) effectively create a "passband" that allows resolution of the ^{39}K hyperfine structure.

This work was supported by ONR Grant No. N00014-90-J-1475 and the Firm J. F. Clauser & Assoc., Walnut Creek, CA. The authors wish to thank M. Reinsch, G. Garfein, and the staff and students at the UC Berkeley Microstructures Laboratory for their assistance.

[1] W. Heisenberg, Z. Phys. **43**, 172 (1927); J. A. Wheeler and W. H. Zurek, *Quantum Theory and Measurement* (Princeton University Press, Princeton, 1983), p. 62.

[2] D. Walls *et al.*, in *Foundations of Quantum Mechanics,* edited by T. D. Black *et al.* (World Scientific, Singapore, 1992), p. 157.

[3] O. Carnal and J. Mlynek, Phys. Rev. Lett. **66**, 2689 (1991); F. Shimizu *et al.*, Phys. Rev. A **46**, R17 (1992).

[4] J. F. Clauser and S. Li, Phys. Rev. A **49**, R2213 (1994); S. Li and J. F. Clauser, *ibid.* **49**, 2702 (1994).

[5] D. W. Keith *et al.*, Phys. Rev. Lett. **66**, 2693 (1991); M. Kasevich and S. Chu, *ibid.* **67**, 181 (1991); F. Riehle *et al.*, *ibid.* **67**, 177 (1991).

[6] U. Sterr *et al.*, Appl. Phys. Lett. B **54**, 341 (1992).

[7] J. F. Clauser and M. W. Reinsch, Appl. Phys. B **54**, 380 (1992).

[8] A. Einstein, Phys. Z. **18**, 121 (1917); B. L. van der Waerden, *Sources of Quantum Mechanics* (Dover, New York, 1968), p. 63.

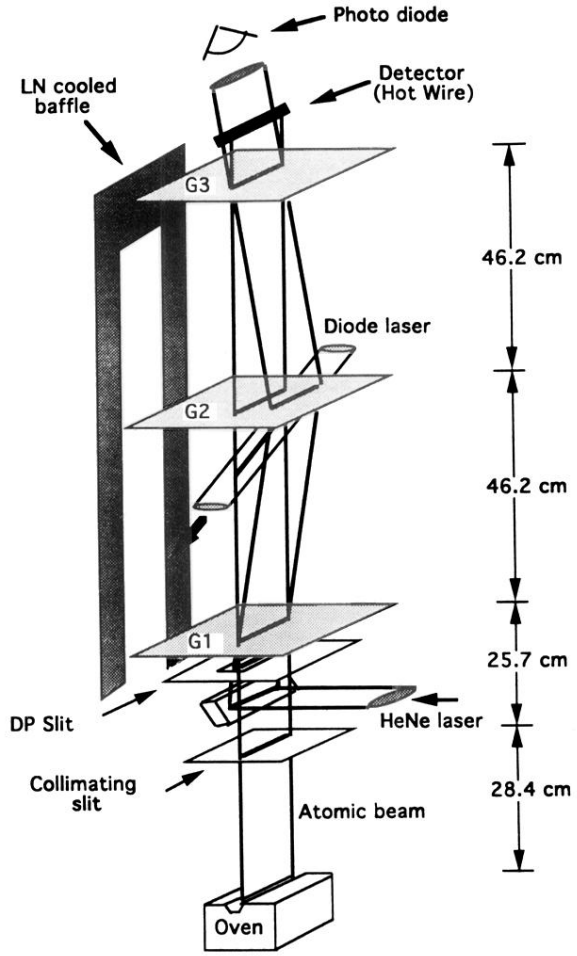

FIG. 1. Geometry of the experimental apparatus. The photomultiplier to measure fluorescence intensity is not shown.

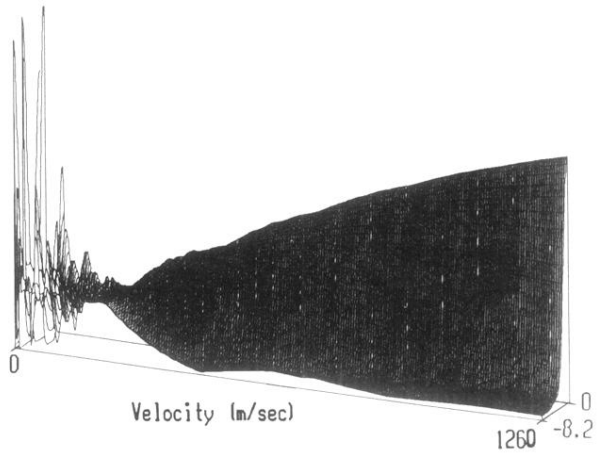

FIG. 2. Calculated laser-off interferometer transmission probability plotted as a function of atomic velocity and grating displacement. The periodic dependence on displacement is plotted through one-half of a geometric-shadow spacing period.

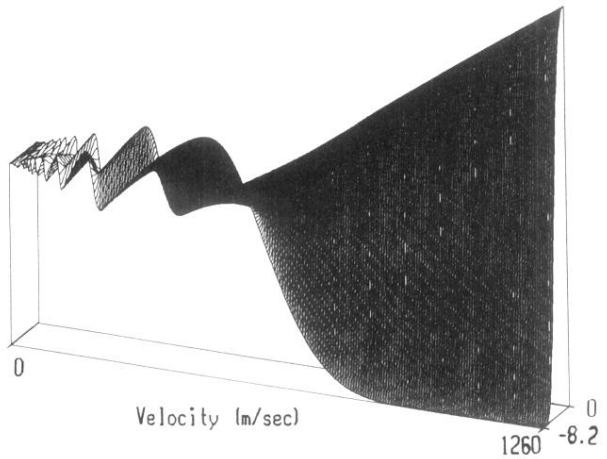

FIG. 3. Calculated laser-on interferometer transmission probability, given the scattering of one photon near G_2, plotted with the format of Fig. 2.